Prepublished Copy

NATURE ENVIRONMENT AND POLLUTION TECHNOLOGY

Article In Press

PEER-REVIEWED PREPUBLISHED MANUSCRIPT

This is a peer-reviewed prepublished version of the paper to be published in **Vol. 26, No. 1, March 2027.**

Congo Red Dye Biosorption Using Bacillus cereus MW13 Isolated from the Wastewater of a Mulberry Paper Mill

Suchanya Thongkrua, Thanyaphon Tharak and Palinee Kaewkampol

RECEIVED
24 May 2026

CITE THIS ARTICLE

Thongkrua, S., Tharak, T. and Kaewkampol, P., 2027. Congo Red Dye Biosorption Using Bacillus cereus MW13 Isolated from the Wastewater of a Mulberry Paper Mill. *Nature Environment and Pollution Technology*, 26(1), D1943.

https://doi.org/10.46488/NEPT.2027.v26i01.D1943

EARLY-ACCESS STATEMENT

This manuscript, after peer review, is being released online in its original, unedited form to provide early access to its findings. Prior to final publication, it will undergo additional editing and formatting. Readers may note that, as an unedited version, the manuscript may have linguistic and other minor errors. The DOI will be active after the final publication of the paper.

PUBLICATION STATUS

PEER REVIEW	ONLINE VERSION	FINAL ISSUE
Completed	**Prepublished**	**March 2027**

© The Author(s) 2027. This article is Open Access under the Creative Commons Attribution 4.0 International License, allowing use, sharing, adaptation and reproduction with proper credit. Images or third-party material are covered by this licence unless otherwise noted. For uses beyond the licence, permission must be obtained from the copyright holder. Licence details: creativecommons.org/licenses/by/4.0/.

Congo Red Dye Biosorption Using *Bacillus cereus* MW13 Isolated from the Wastewater of a Mulberry Paper Mill

Suchanya Thongkrua†, Thanyaphon Tharak and Palinee Kaewkampol

School of Energy and Environment, University of Phayao, Phayao, Thailand; suchanya.th@up.ac.th
†Corresponding author: Suchanya Thongkrua; suchanya_9@yahoo.com

Abstract

The untreated Congo red discharge from the textile and paper industries has several impacts on humans, including carcinogenic and mutagenic effects, as well as on aquatic life and the environment. The current study investigated the biosorption performance of dye-tolerant bacteria for the removal of Congo red under various factors. *Bacillus cereus* MW13 was isolated from the wastewater of a mulberry paper mill in Northern Thailand. The optimum conditions were a Congo red initial concentration of 600 $mg.L^{-1}$, a biomass concentration of 4 $g.L^{-1}$, and a contact time of 240 min, resulting in the maximum removal efficiency of 90.24±0.11%. The highest biosorption capacity, 367.52±8.93 $mg.g^{-1}$, was achieved at a biomass concentration of 0.5 $g.L^{-1}$. The biosorption isotherm and kinetic analysis were best fit by the Langmuir model (R^2=0.9852) and the pseudo-second-order model (R^2=0.9994), respectively. SEM and TEM analyses following Congo red exposure showed the deposition of dye molecules on the cell surface, accompanied by a thicker cell wall and increased cytoplasmic electron density. Furthermore, the functional groups of *B. cereus* MW13 after Congo red exposure, including the hydroxyl, amino, and carboxyl groups, as well as the S=O stretching of the Congo red molecule, were detected by FTIR analysis. It revealed that a binding interaction between Congo red molecules and functional groups on the cell surface occurred during the biosorption process. These results confirmed the potential of *B. cereus* MW13 biomass for Congo red biosorption.

Keywords
Bacillus cereus; Congo red dye; Biosorption isotherms; Biosorption kinetics

1. INTRODUCTION

Congo red is water-soluble and classified as an anionic (acid) dye (Ellafi et al. 2023). Based on its structure, consisting of two chromophore groups (-N=N-), it belongs to the azo dye class (Goud et al. 2020, Abubakar et al. 2023, Singh et al. 2024, Strebel et al. 2024). Congo red can be applied to cotton, silk, and wood (Rane & Joshi 2021), and is used extensively in textiles, as a food colorant, and in paper printing (Singh & Dwivedi 2020). Due to Congo red' s complex structure, which contains chromophore groups and many aromatic rings, it is highly stable and highly resistant to biodegradation (Goud et al. 2020, Harja et al. 2022, Strebel et al. 2024). Consequently, Congo red has been reported to cause damage to aquatic life, humans, and the environment. Its toxicity is recognized for carcinogenic and mutagenic effects, as well as for skin and eye irritation (Singh & Dwivedi 2020, Harja et al. 2022). Congo red effluent contamination of natural aquatic systems leads to elevated BOD and COD levels, reduced photosynthesis and dissolved oxygen concentrations, and aesthetic problems (Goud et al. 2020, Bhayana et al. 2023, Kumar et al. 2025). Hence, an effective removal of Congo red effluent is necessary.

Traditional biological treatment has not been appropriate for azo dye remediation because of its low efficiency (Didier de Vasconcelos et al. 2021). Moreover, some physical and chemical procedures face challenges due to limitations such as complex steps, high operational costs, and non-eco-friendly practices (Bhayana et al. 2023, Abubakar et al. 2023). Therefore, alternative bioremediation methods have been applied to remove azo dyes from aquatic solutions. Biosorption is a bioremediation process that involves adsorption, surface complexation, ion exchange, and precipitation (Goud et al. 2020, Abubakar et al. 2023). Therefore, the biosorption technique usually provides high performance, a quick process, ease of use, low cost, and environmental friendliness (Abubakar et al. 2023). Previous studies have been conducted to determine the bioremediation efficiency of Congo red using B. cereus, with removal efficiencies ranging from 21-40% within 4 days (Alhefeiti et al. 2021). Khudhair & Al-Fayaad (2022) confirmed the removal of 100 ppm Congo red, achieving 92.9% removal efficiency under optimal conditions after 3 days. In the case of dye biosorption using Bacillus sp. biomass. Sarim et al. (2019) reported that *B. subtilis* HAU-KK01

efficiently decolorized Congo red within a short time. Chemisorption was predicted to be the main mechanism in the biosorption. In addition, the study of Acridine orange dye biosorption utilizing *B. cereus* M^{1}_{16} was presented by Bag et al. (2021). The maximum capacity was 210.46 $mg.g^{-1}$ at pH 7 and 30 °C within 300 min. The biosorption kinetics were best fit by the pseudo-second order.

In Northern Thailand, Congo red is commonly used in mulberry paper mills. The untreated effluent is discharged into the aquatic environment. The present research aims to investigate the performance of *B. cereus* MW13, an isolate from a mulberry paper mill wastewater in northern Thailand, in removing Congo red. The study focused on the biosorption process and the effects of factors on the removal efficiency and capacity. Furthermore, the surface morphology, the internal structure, and functional groups of bacterial biomass were identified to explain the biosorption mechanism.

2. MATERIALS AND METHODS

2.1 Preparation of Bacterial Biomass

B. cereus MW13, a local Congo red-tolerant bacterium, was isolated from the wastewater at the mulberry paper mill in northern Thailand. Bacterial identification of isolate MW13 was performed by the National Center for Genetic Engineering and Biotechnology, Thailand, using single-stranded 16S rDNA sequencing, which showed 100% similarity to *B. cereus*. The nutrient broth medium was composed of 5 g peptone, 5 g sodium chloride, 1.5 g HM peptone B, and 1.5 g yeast extract. 13 g of the medium was dissolved in 1000 mL of distilled water. *B. cereus* MW13 was grown in a nutrient broth medium and cultivated in a shaking incubator at 120 rpm and 30 °C for 24 hr. Bacterial suspensions were collected using centrifugation at 8,000 rpm for 30 min. The bacterial biomass was washed three times with sterile deionized water and dried at 40 °C before experimentation.

2.2 Congo Red Biosorption Experiments

The effects of different initial Congo red concentrations (200, 400, 600, 800 and 1,000 $mg.L^{-1}$), biomass concentrations (0.5, 1, 2, 3 and 4 $g.L^{-1}$), and contact times (5, 10, 15, 20, 25, 30, 45, 60, 120, 240, 360 and 480 min) on the removal efficiency and biosorption capacity of Congo red were determined. Biosorption experiments were conducted in batch and performed in triplicate. Dye solution was prepared using Congo red ($C_{32}H_{22}N_6Na_2O_6S_2$) for microscopy (Loba Chemie, India). The biomass of *B. cereus* MW13 was resuspended in a 100 mL Congo red solution (initial pH: 8.17-9.13) at room temperature and shaken at 120 rpm. The suspension was then centrifuged at 8,000 rpm for 10 min. The residual dye concentration in the supernatant was measured using a Shimadzu UV-Visible Spectrophotometer (AA-6880) at 495 nm. The surface morphology of *B. cereus* MW13 before and after biosorption was analyzed by Scanning Electron Microscopy (SEM) using a JEOL JEM-IT300 instrument. A Transmission Electron Microscope (TEM) of the Talos F200X model was used to study the characteristics of intracellular bacteria. In addition, Fourier Transform Infrared Spectroscopy (FTIR) was performed to identify functional groups in *B. cereus* MW13 biomass using a Thermo Scientific spectrometer (Nicolet iS5) over the wavenumber range of 4,000-400 cm^{-1}. After the experiment, the dye-loaded biomass was sterilized by autoclaving at 121°C under 15 psi for 30 minutes to eliminate any viable bacterial cells. Following sterilization, the biomass was disposed of through the University of Phayao's waste management system in accordance with the University's waste disposal procedures. Removal efficiency and biosorption capacity of Congo red were calculated using Equations (1) and (2), respectively:

$$\text{Removal efficiency (\%)} = \frac{C_0 - C_t}{C_0} \times 100 \quad \ldots(1)$$

$$q_e = \frac{C_0 - C_e}{M} \times V \quad \ldots(2)$$

where C_0 and C_t represent the concentrations of Congo red at the initial time ($mg.L^{-1}$) and at time t (min), respectively; q_e means the equilibrium biosorption capacity ($mg.g^{-1}$), and C_e is the residual concentration of Congo red at equilibrium time ($mg.L^{-1}$). V and M are the total volume of the suspension (L) and the dry biomass in the suspension (g), respectively (Bag et al. 2021, Thongkrua & Kasuya 2023, Alamri et al. 2025).

The biosorption isotherms were assessed using the Langmuir and the Freundlich models to analyze the biosorption process of Congo red onto a biomass surface, given by linear Equations (3) and (4), respectively:

$$\frac{C_e}{q_e} = \frac{1}{K_L q_m} + \frac{C_e}{q_m} \quad \ldots(3)$$

$$lnq_e = lnK_F + \frac{1}{n} lnC_e \quad \ldots(4)$$

In the case of the Langmuir model, the value of R_L indicated the shape of the Langmuir isotherm and the nature of the biosorption process, which are expressed in Equation (5):

$$R_L = \frac{1}{1 + K_L C_0} \quad \ldots(5)$$

where q_m is defined as the maximum specific uptake ($mg.g^{-1}$), and K_L means the Langmuir constant, which pertains to the affinity of the binding sites ($L.mg^{-1}$). K_F denotes the adsorption capacity for the Freundlich isotherm, while the adsorption intensity is identified by n (Wu et al. 2020, Thongkrua & Kasuya 2023, Alamri et al. 2025).

The biosorption kinetics of Congo red were determined to predict the biosorption rate and evaluate the mechanism of pollutant uptake by the pseudo-first-order kinetic model, the pseudo-second-order kinetic model, and the intraparticle diffusion model, which can be described in linear form by following Equations (6), (7), and (8), respectively:

$$log(q_e - q_t) = logq_{ecal} - \frac{k_1}{2.303} t \quad \ldots(6)$$

$$\frac{t}{q_t} = \frac{1}{k2^2 qecal^2} + \frac{1}{q_{ecal}} t \quad \ldots(7)$$

$$q_t = k_i t^{1/2} + C \quad \ldots(8)$$

where q_t is the biosorption capacity ($mg.g^{-1}$) at time t (min). q_{ecal} is the calculated equilibrium biosorption capacity ($mg.g^{-1}$). k_1, k_2, and k_i represent the rate constants for the pseudo-first-order kinetic model (min^{-1}), the pseudo-second-order kinetic model ($g.mg^{-1}.min^{-1}$), and the intraparticle diffusion model ($mg.g^{-1}.min^{-1/2}$), respectively, while C is the constant associated with diffusion boundary layer thickness ($mg.g^{-1}$) (Wu et al. 2020, Bag et al. 2021, Thongkrua & Kasuya 2023, Alamri et al. 2025).

3. RESULTS AND DISCUSSION

3.1 Effects of Initial Congo Red Concentration

The effects of initial Congo red concentration (200-1,000 $mg.L^{-1}$) on Congo red biosorption using *B. cereus* MW13 were investigated with an equilibrium time of 240 min for 200-600 $mg.L^{-1}$ and 360 min for 800-1,000 $mg.L^{-1}$, and a bacterial biomass of 2 $g.L^{-1}$. Fig. 1(a) shows that at initial concentrations of 400 $mg.L^{-1}$ and 600 $mg.L^{-1}$, *B. cereus* MW13 exhibited similar Congo red removal efficiencies, achieving 64.04±0.21% and 62.32±0.31%, respectively. The trend showed that Congo red removal efficiency decreased as initial concentration increased. Congo red biosorption depended on hydrogen bonding between the anionic dye's

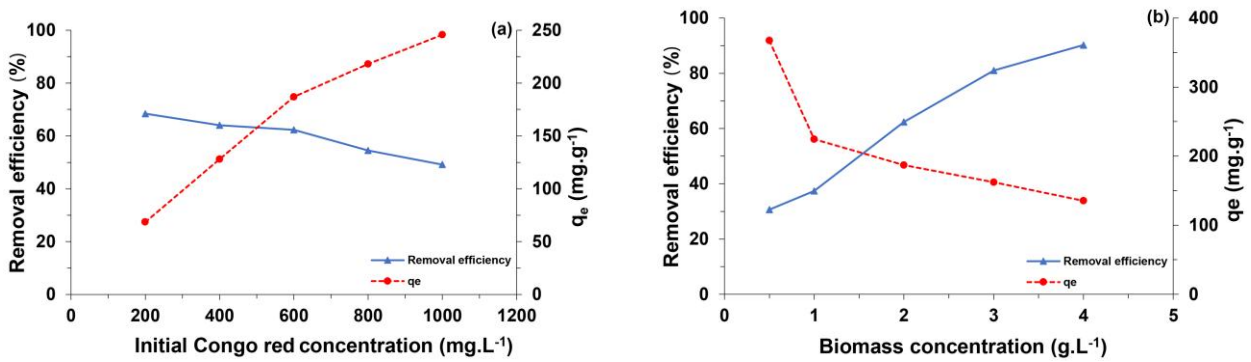
negative charge (SO_3^-) (Goud et al. 2020, Singh et al. 2024) and functional groups, such as -NH, -COOH, and -OH, in peptidoglycan, the cell wall of *B. cereus* (Bag et al. 2021, Li et al. 2023). Insufficient bacterial biomass and a high Congo red concentration can saturate binding sites, thereby decreasing removal efficiency (Strebel et al. 2024). In addition, the findings can be attributed to the elevated Congo red concentration, which led to dye toxicity (Haque et al. 2021). A similar result was observed in previous studies using *B. cereus* (Khudhair & Al-Fayaad 2022) and *Bacillus sp.* (Sonwani et al. 2020, Haque et al. 2021). In contrast, the biosorption capacity at an initial Congo red concentration of 1,000 mg.L^{-1} was 245.76±1.11 mg.g^{-1}, the maximum. This results from increased dissociation of the anionic Congo red dye, enhanced diffusion rate, and a greater number of dye molecules, leading to greater competition and interaction for available active sites on the bacterial surface at elevated Congo red concentrations (Harja et al. 2022, Strebel et al. 2024).

3.2 Effects of Biomass Concentration

The influences of *B. cereus* MW13 biomass concentration (0.5-4 g.L^{-1}) on Congo red biosorption were observed under an initial dye concentration of 600 mg.L^{-1} at an equilibrium time of 240 min, as illustrated in Fig. 1(b). As bacterial biomass rose from 0.5 to 4 g.L^{-1}, the effectiveness of Congo red elimination correspondingly improved. The maximum removal efficiency of 90.24±0.11% was achieved at the highest biomass. This results in hydrogen bonding, increasing the cell surface area available to Congo red molecules during biosorption, which is elevated with the augmentation of bacterial biomass (Wang et al. 2021). A similar effect of biomass quantity on Congo red removal by *B. haynesii* ING6 has been identified by Dharsandia et al. (2025). The biosorption capacity decreased as the biomass concentration increased. The maximum biosorption capacity of 0.5 g.L^{-1} biomass was 367.52±8.93 mg.g^{-1}. This behavior can be explained by the available dye molecules failing to adequately cover the binding site on the cell surface at high biomass concentration (Zhang & Huang 2020).

3.3 Effects of Contact Time

The influences of contact time (5-480 min) on Congo red biosorption were investigated using *B. cereus* MW13 biomass at 4 g.L^{-1} and Congo red solution at 600 mg.L^{-1}, as presented in Fig. 1(c). Biosorption of Congo red occurred rapidly during the initial phase (0-30 min) and then gradually increased until equilibrium was attained. In the early period of the contact, Congo red degradation occurred via biosorption, driven by the abundance of empty active binding sites on the bacterial cell surface and by fast diffusion to the cell surface (Semwal et al. 2023). Subsequently, the biosorption rate decreases due to saturation of binding sites (Zhang & Huang 2020, Bag et al. 2021). At an equilibrium time of 240 min, the removal efficiency and biosorption capacity were determined at 90.24±0.11% and 135.36±0.19 mg.g^{-1}, respectively. Related research on the removal of Reactive Black 5 dye by the *B. cereus* strain KM201428 reported that removal efficiency increased with increasing contact time, reaching an optimum at 120 hr, with over 97% (Wanyonyi et al. 2019). Furthermore, Thakur et al. (2018) demonstrated that *B. cereus* MSS2.8 and bioiron nanoparticles achieved a Congo red removal efficiency of 98.7% at an initial concentration of 20 mg.L^{-1} within 32 hr.



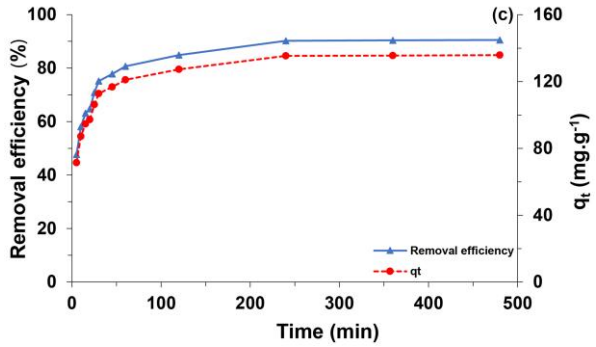


Fig. 1: Effects of initial Congo red concentration (a), biomass concentration (b), and time (c) on Congo red biosorption.

3.4 Biosorption Isotherms

The biosorption isotherms, including the Langmuir and the Freundlich models, were used to describe the mechanism of Congo red adsorption on the *B. cereus* MW13 surface and to determine the equilibrium adsorption capacity at 240 min, as shown in Table 1. In addition, Fig. 2(a) and 2(b) illustrate the Langmuir and the Freundlich equations, respectively. The theoretical data fit the Langmuir model, as indicated by the highest linear correlation coefficient (R^2). It reveals that Congo red was adsorbed onto the homogeneous bacterial surface via monolayer biosorption (Alamri et al. 2025), with a high maximum adsorption capacity, resulting in high effectiveness in Congo red removal using *B. cereus* MW13. Furthermore, the R_L values ranged from 0 to 1, confirming that the biosorption conditions were appropriate. Bag et al. (2021) reported similar experimental data on the biosorption isotherm of the organic dye Acridine orange utilizing *B. cereus* $M^1{}_{16}$.

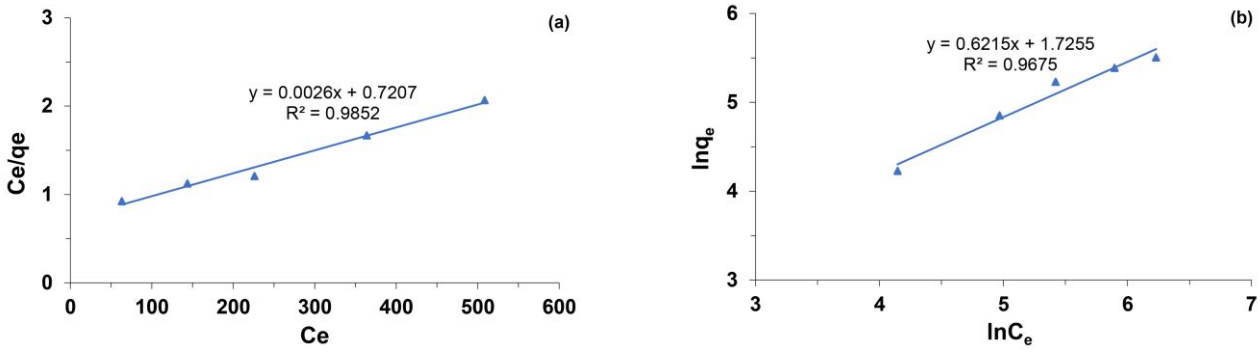


Fig. 2: Congo red biosorption isotherms: Langmuir (a)

and Freundlich (b) isotherms.

Table 1: Congo red biosorption isotherm parameters using *B. cereus* MW13.

Langmuir isotherm				Freundlich isotherm		
q_m (mg.g^{-1})	k_L (L.mg^{-1})	R_L	R^2	n	k_F	R^2
384.62	0.0036	0.32	0.9852	1.61	5.62	0.9675

3.5 Biosorption Kinetics

Biosorption kinetics were utilized to explain the biosorption rate and dynamics of Congo red adsorption by *B. cereus* MW13, including the pseudo-first-order, pseudo-second-order, and intraparticle diffusion models, as shown in Fig. 3(a), 3(b), and 3(c), respectively. The pseudo-second-order kinetic model provided the best fit, with the highest linear correlation coefficient (R^2) and a close match between the calculated q_{ecal} and the experimental q_e, as illustrated in Table 2. This study revealed that Congo red adsorption was a chemisorption process in which the dye anion bound to the bacterial cell surface (Wu et al. 2020). Furthermore, the intraparticle graph did not pass through the origin, indicating the absence of intraparticle diffusion. According to a previous study, the pseudo-second-order kinetic model was the best-fit model for Congo red biosorption using *B. subtilis* HAU-KK01 (Sarim et al. 2019) and *B. subtilis*-CuO nanocomposite (Alamri et al. 2025), and for the organic dye Acridine orange using *B. cereus* M^{1}_{16} (Bag et al. 2021).

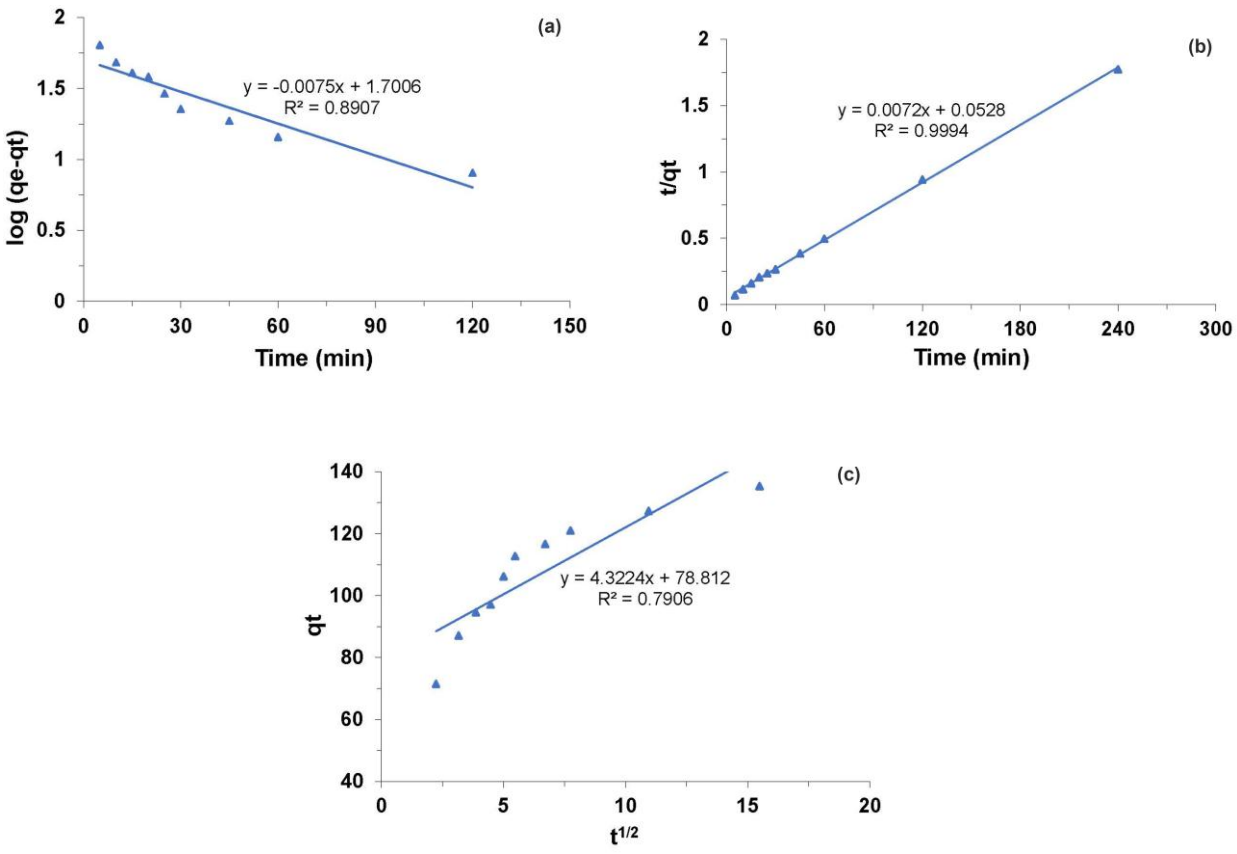


Fig. 3: Kinetic model for Congo red biosorption: Pseudo-first-order kinetic (a), Pseudo-second-order kinetic (b), and Intraparticle diffusion (c).

Table 2: Kinetic model parameters for Congo red biosorption using *B. cereus* MW13.

Biosorption kinetic models	Parameters	Values
Pseudo-first-order kinetic model	q_{ecal} ($mg.g^{-1}$)	50.19
	k_1 (min^{-1})	0.0173

	R^2	0.8907
Pseudo-second-order kinetic model	q_{ecal} ($mg.g^{-1}$)	138.89
	k_2 ($g.mg^{-1}.min^{-1}$)	0.0313
	R^2	0.9994
Intraparticle diffusion model	k_i ($mg.g^{-1}.min^{-1/2}$)	4.3224
	C ($mg.g^{-1}$)	78.81
	R^2	0.7906

3.6 SEM and TEM Analysis

The surface morphological characterizations of *B. cereus* MW13 before and after Congo red removal at an initial concentration of 600 $mg.L^{-1}$, at the optimum of 240 min, were performed by SEM, as shown in Fig. 4. Before treatment (Fig. 4(a)), the bacterial cells were rod-shaped with a smooth cell surface. In contrast, after dye treatment (Fig. 4(b)), the cell surface was rough, and Congo red appeared to adhere to it. The wrinkling of the bacterial cell surface was likely due to chemical interactions between the anionic components of the Congo red and functional groups of the bacterial cell wall (Othman et al. 2025). Similarly, *B. cereus* morphology has been observed in related studies (Diao et al. 2018, Park et al. 2019, Bag et al. 2021, Li et al. 2023).

In addition, the internal structure of *B. cereus* MW13 before and after Congo red remediation is presented in Fig. 5. The TEM micrograph of an untreated cell showed an intact cell wall and uniformly distributed cytoplasm (Fig. 5(a)). After 240 min of Congo red exposure (Fig. 5(b)), the cell wall was thicker, and numerous dark inclusion bodies were present in the cytoplasm. These observations indicated that the apparent thickening of the cell wall may result from the binding of Congo red molecules to the cell surface and cell wall functional groups (Pi et al. 2022).

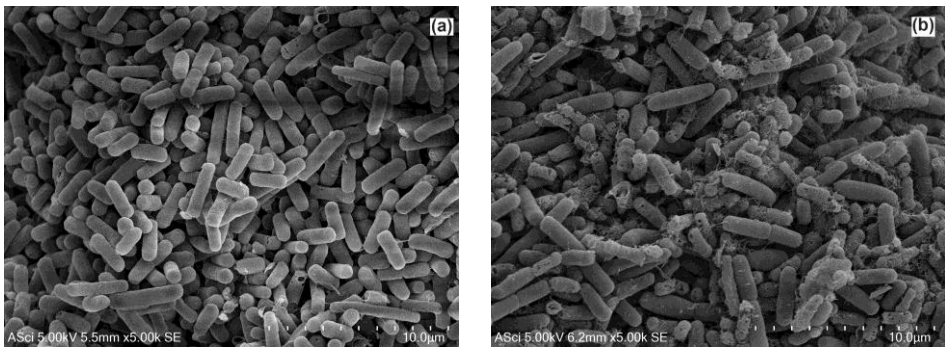


Fig. 4: SEM micrographs of *B. cereus* MW13 before (a) and after (b) Congo red biosorption.

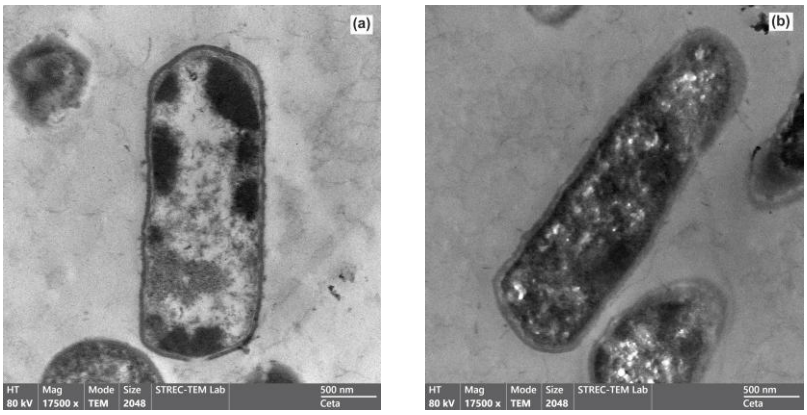


Fig. 5: TEM micrographs of *B. cereus* MW13 before (a) and after (b) Congo red biosorption.

3.7 FTIR Analysis

The functional groups of the *B. cereus* MW13 cell surface before and after Congo red treatment were identified by FTIR, as illustrated in Fig. 6. Before dye exposure, the broad peak at 3289.48 cm^{-1} presented the stretching vibration of the O-H group in polysaccharides. C-H stretching vibrations (alkane) of the methyl and methylene groups were detected at 2961.16 cm^{-1} and 2929.34 cm^{-1}, respectively. The weak to medium peaks at 2359.96 cm^{-1} and 2342.12 cm^{-1} were attributed to C≡N stretching (nitrile) and C≡C stretching (alkyne), respectively. The C=O stretching (amide or carboxyl group) and C=C stretching (alkene) appeared as strong peaks at 1652.21 cm^{-1} and 1540.85 cm^{-1}, respectively. Other medium peaks were detected at 1453.10 cm^{-1}, 1231.81 cm^{-1}, and 1044.27 cm^{-1}, which were assigned to the stretching vibrations of C-H bending, C-N stretching (amide Ⅲ), and C-O-C stretching vibration in polysaccharides on the bacterial cell wall (Gao et al. 2022, Shandookh, 2025), respectively. The related studies reported similar functional groups on the *B. cereus* cell surface, including proteins, lipids, and carbohydrates (Bag et al. 2021, Silfiani et al. 2022, Li et al. 2023, Othman et al. 2025). After dye exposure, the main functional groups were shifted, resulting in decreased band intensity and changes in peak shape. The new vibration peak at 1056.80 cm^{-1} was assigned to S=O stretching of the Congo red molecule (Ellafi et al. 2023). These results revealed that surface binding between Congo red molecules and cell-surface functional groups occurred during biosorption.

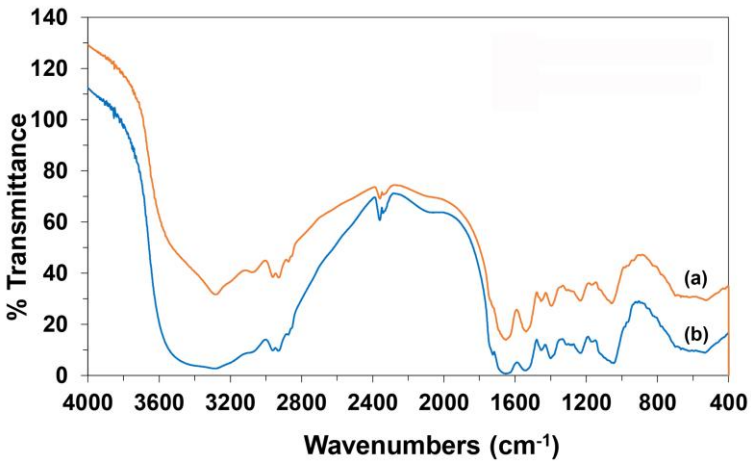


Fig. 6: FTIR spectra of *B. cereus* MW13 before (a) and after (b) Congo red biosorption.

4. CONCLUSIONS

The study determined the effects of various factors on the biosorption performance of Congo red dye using *B. cereus* MW13, isolated from mulberry paper mill wastewater in Northern Thailand. At suitable initial dye concentrations, increasing biomass concentration and contact time led to higher removal efficiency. The maximum biosorption capacity was achieved at 367.52±8.93 $mg.g^{-1}$. At the equilibrium time (240 min), monolayer adsorption onto homogeneous binding sites was described by the Langmuir model, and the biosorption process followed chemisorption on the cell surface, as indicated by the pseudo-second-order kinetic model and the absence of intraparticle diffusion. In addition, SEM and TEM micrographs obtained after Congo red exposure revealed the deposition of dye molecules on the bacterial cell surface, together with an apparent thickening of the cell wall and increased electron density within the cytoplasm. The functional groups of bacterial cells, identified by FTIR, were responsible for active binding sites for Congo red molecule adsorption. The results provide essential baseline data for future studies on the treatment of actual mulberry paper mill wastewater. Future studies should investigate key operational parameters (pH, temperature, salinity, ionic strength, and competing contaminants) and the toxicity of the treated dye solution to verify the practical applicability and environmental sustainability of the biosorption process.

5. ACKNOWLEDGMENTS

This research was supported and funded by University of Phayao and Thailand Science Research and Innovation Fund (Fundamental Fund 2025, Grant No. 5125/2567).

6. REFERENCES

Abubakar, A., Yasid, N.A., Othman, A.R. and Shukor, Y., 2023. Biosorption of azo dyes by bacterial biomass: a review. *Journal of Environmental Microbiology and Toxicology*, 11(1), pp.38-51.

Alamri, T., Mokhtar, J.A., Hassan, E.A., Harakeh, S., Niyazi, H.A., Niyazi,H.A., Abujamel, T., Alrasheedi, H., Chehab, N.A. and El-Aal,M.A., 2025. *Bacillus subtilis*-CuO nanocomposites as a sustainable solution for congo red dye remediation: adsorption studies and kinetic modeling. *Egyptian Journal of Aquatic Research*, 51(4), pp.453-462.

Alhefeiti, M.A., Athamneh, K., Vijayan, R. and Ashraf, S.S., 2021. Bioremediation of various aromatic and emerging pollutants by *Bacillus cereus* sp. isolated from petroleum sludge. *Water Science & Technology*, 83(7), pp.1535-1547.

Bag, S., Hasan, M.I., Halder, D. and Ghosh, A., 2021. Biosorption of organic dye acridine orange from aqueous solution using dry biomass of *Bacillus cereus* $M1_{16}$. *Archives of Microbiology*, 203, pp.3811–3823.

Bhayana, T., Saxena, A., Gupta, S. and Dubey, A.K., 2023. Enhanced decolourisation and degradation of azo dyes using wild versus mutagenic improved bacterial strain: a review. *Vegetos*, 36, pp.28–37.

Dharsandia, I., Kumar, N., Tiwari, A. and Parmar, P., 2025. Enhanced decolorization of congo red and methyl orange using *Bacillus haynesii* ING6: an optimization study using central composite design (CCD). *Biodegradation*, 36(121), pp.1-16.

Diao, M., Qi, D., Xu, M., Lu, Z., Lv, F., Bie, X., Zhang, C. and Zhao, H., 2018. Antibacterial activity and mechanism of monolauroyl-galactosylglycerol against *Bacillus cereus*. *Food Control*, 85, pp.339-344.

Didier de Vasconcelos, G.M., Mulinari, J., de Arruda Guelli Ulson de Souza, S.M., Ulson de Souza, A.A., de Oliveira, D. and de Andrade, C.J., 2021. Biodegradation of azo dye-containing wastewater by activated sludge: a critical review. *World Journal of Microbiology and Biotechnology*, 37, p.101.

Ellafi, A., Dali, A., Mnif. S. and Younes, S.B., 2023. Microbial enzymatic degradation, spectral analysis and phytotoxicity assessment of congo red removal by *Bacillus spp. Catalysis Letters*, 153, pp.3620–3633.

Gao, Z., Yang, J., Wu, J., Li, H., Wu, C., Yin, Z., Xu, J., Zhu, L., Gao, M. and Zhan, X., 2022. Structural characterization and in vitro evaluation of the prebiotic potential of an exopolysaccharide produced by *Bacillus thuringiensis* during fermentation. *LWT-Food Science and Technology*, 163, p.113532.

Goud, B.S., Cha, H.L., Koyyada, G. and Kim, J.H., 2020. Augmented biodegradation of textile azo dye effluents by plant endophytes: a sustainable, eco-friendly alternative. *Current Microbiology*, 77, pp.3240–3255.

Haque, M.M., Haque, M.A., Mosharaf, M.K. and Marcus, P.K., 2021. Novel bacterial biofilm consortia that degrade and detoxify the carcinogenic diazo dye congo red. *Archives of Microbiology*, 203(2), pp.643-654.

Harja, M., Buema, G. and Bucur, D., 2022. Recent advances in removal of congo red dye by adsorption using an industrial waste. *Scientific Reports*, 12, p.6087.

Khudhair, S.H. and Al-Fayaad, D.B.M., 2022. Bacterial biodegradation of congo red dye using local bacterial isolates. *Iraqi Journal of Science,* 63(11), pp.4674-4682.

Kumar, M., Mishra, A., Patel, S.K., Kushwaha, J., Singh, S., Mishra, V., Singh, D., Singh, V., Giri, B.S., Singhania, R.R. and Singh, D., 2025. Environmental impacts and strategies for bioremediation of dye-containing wastewater. *Bioengineering*, 12(10), p.1043.

Li, Q., Zhang, W., Liao, S., Xing, D., Xiao, Y., Zhou, D. and Yang, Q., 2023. Mechanism of lead adsorption by a *Bacillus cereus* strain with indole-3-acetic acid secretion and inorganic phosphorus dissolution functions. *BMC Microbiology*, 23(1), p.57.

Othman, A.R., Imron, M.F., Ismail, N.'I., Kamaruzzaman, M.A., Abdullah, S.R.S., Al-Baldawi, I.A., Kurniawan, S.B., Jusoh, H.H.W., Ismail, A. and Hasan, H.A., 2025. Biosorption of hexavalent chromium in aqueous solution by *Bacillus cereus. Environmental Technology & Innovation*, 37, p.104015.

Park, E., Hussain, M.S., Wei, S., Kwon, M. and Oh, D., 2019. Genotypic and phenotypic characteristics of biofilm formation of emetic toxin producing *Bacillus cereus* strains. *Food Control*, 96, pp.527-534.

Pi, Y., Duan,C., Zhou,Y., Sun, S., Yin, Z., Zhang, H., Liu, C. and Zhao, Y. (2022). The effective removal of Congo Red using a bio-nanocluster: Fe_3O_4 nanoclusters modified bacteria. *Journal of Hazardous Materials*, 424, p.127577.

Rane, A. and Joshi, S.J., 2021. Biodecolorization and biodegradation of dyes: a review. *The Open Biotechnology Journal*, 15(1), pp.97-108.

Sarim, K.M., Kukreja, K., Shah, I. and Choudhary, C.K., 2019. Biosorption of direct textile dye congo red by *Bacillus subtilis* HAU-KK01. *Bioremediation Journal*, 23(3), 185-195.

Semwal, N., Mahar, D., Chatti, M., Dandapat, A. and Arya, M.C., 2023. Adsorptive removal of congo red dye from its aqueous solution by Ag–Cu–CeO_2 nanocomposites: adsorption kinetics, isotherms, and thermodynamics. *Heliyon*, 9(11), p.e22027.

Shandookh, F.K., 2025. FTIR characterization of biosurfactants that produced from *Bacillus subtilis* isolated from wastewater samples contaminated with organic pollutants. *International Journal of Chemical and Biological Sciences*, 7(2), pp.102-105.

Silfiani, I., Abadi, A.L., Aini, L.Q., Prillianti, K.R., Prabowo, M.R. and Dianti, S.H., 2022. FTIR (Fourier Transform Infrared) Spectroscopy method for *Bacillus cereus* characterization. *Research Journal of Life Science*, 9(2), pp.69-76.

Singh, G. and Dwivedi, S.K., 2020. Decolorization and degradation of direct blue-1 (azo dye) by newly isolated fungus *Aspergillus terreus* GS28, from sludge of carpet industry. *Environmental Technology & Innovation*, 18, p.100751.

Singh, G.B., Vinayak, A., Mudgal, G. and Kesari, K.K., 2024. Azo dye bioremediation: an interdisciplinary path to sustainable fashion. *Environmental Technology & Innovation*, 36, p.103832.

Sonwani, R.K., Swain, G., Giri, B.S., Singh, R.S. and Rai, B.N., 2020. Biodegradation of congo red dye in a moving bed biofilm reactor: performance evaluation and kinetic modeling. *Bioresource Technology*, 302, p.122811.

Strebel, A., Behringer, M., Hilbig, H., Machner, A. and Helmreich, B., 2024. Anionic azo dyes and their removal from textile wastewater through adsorption by various adsorbents: a critical review. *Frontiers in Environmental Engineering*, 3, p.1347981.

Thakur, P., Kashyap, P., Sharma, H. and Shirkot, P., 2018. In-vitro effect of bacterial culture of *Bacillus cereus* MSS 2.8 and bioiron nanoparticles synthesized by *Bacillus cereus* MSS 2.8 on decolorization of textile dyes. *International Journal of Chemical Studies*, 6(5), pp.3450-3454.

Thongkrua, S. and Kasuya, A., 2023. Utilization of *Enterobacter cloacae* WW1 biomass for biosorption of lead (II) from aqueous solution. *Nature Environment and Pollution Technology*, 22(1), pp.261-268.

Wang, A., Liu, C., Ge, X., Meng, W., Pi, Y. and Liu, C., 2021. Enhanced removal of congo red dye from aqueous solution by surface modified activated carbon with bacteria. *Journal of Applied Microbiology*, 131(5), pp.2270-2279.

Wanyonyi, W.C., Onyari, J.M., Shiundu, P.M. and Mulaa, F.J., 2019. Effective biotransformation of reactive black 5 dye using crude protease from *Bacillus cereus* strain KM201428. *Energy Procedia*, 157, pp.815-824.

Wu, K., Pan, X., Zhang, J., Zhang, X., zene S.A. and Tian, Y., 2020. Biosorption of congo red from aqueous solutions based on self-immobilized mycelial pellets: kinetics, isotherms, and thermodynamic studies. *ACS Omega*, 5(38), pp.24601-24612.

Zhang, W. and Huang, Y., 2020. The synthesis of PbS NPs and biosorption of Pb(II) by *Shinella zoogloeoides* PQ7 in aqueous conditions. *Water*, 12(7), p.2065.

7. PATENTS

-

8. Description of Abbreviations, if any

-

9. BACKGROUND INFORMATION FOR RECORD (NOT TO BE PRINTED)

Author Contributions: Conceptualization, Suchanya Thongkrua; methodology, Suchanya Thongkrua, Thanyaphon tharak, and Palinee Kaewkampol; formal analysis, Suchanya Thongkrua; investigation, Suchanya Thongkrua; resources, Suchanya Thongkrua; data curation, Suchanya Thongkrua; writing-original draft preparation, Suchanya Thongkrua; writing-review and editing, Suchanya Thongkrua; visualization, Suchanya Thongkrua; project administration, Suchanya Thongkrua; funding acquisition, Suchanya Thongkrua. All authors have read and agreed to the published version of the manuscript."

Institutional Review Board Statement: -

Informed Consent Statement: -

Conflicts of Interest: The authors declare no conflicts of interest. The funders had no role in the design of the study; in the collection, analysis, or interpretation of data; in the writing of the manuscript; or in the decision to publish the results.